THE JOURNAL OF PHYSICAL CHEMISTRY Letters

Letter

pubs.acs.org/JPCL

Use of Surface Photovoltage Spectroscopy to Measure Built-in Voltage, Space Charge Layer Width, and Effective Band Gap in CdSe Quantum Dot Films

Jing Zhao, Benjamin A. Nail, Michael A. Holmes, and Frank E. Osterloh*

Department of Chemistry, University of California, Davis, One Shields Avenue, Davis, California 95616, United States

Supporting Information

ABSTRACT: Surface photovoltage spectroscopy (SPS) was used to study the photochemistry of mercaptoethanol-ligated CdSe quantum dot (2.0−4.2 nm diameter) films on indium doped tin oxide (ITO) in the absence of an external bias or electrolyte. The n-type films generate negative voltages under super band gap illumination (0.1−0.5 mW cm^{-2}) by majority carrier injection into the ITO substrate. The photovoltage onset energies track the optical band gaps of the samples and are assigned as effective band gaps of the films. The photovoltage values (−125 to −750 mV) vary with quantum dot sizes and are modulated by the built-in potential of the CdSe−ITO Schottky type contacts. Deviations from the ideal Schottky model are attributed to Fermi level pinning in states approximately 1.1 V negative of the ITO conduction band edge. Positive photovoltage signals of +80 to +125 mV in films of >4.0 nm nanocrystals and in thin (70 nm) nanocrystal films are attributed to electron−hole (polaron) pairs that are polarized by a space charge layer at the CdSe−ITO boundary. The space charge layer is 70−150 nm wide, based on thickness-dependent photovoltage measurements. The ability of SPS to directly measure built-in voltages, space charge layer thickness, sub-band gap states, and effective band gaps in drop-cast quantum dot films aids the understanding of photochemical charge transport in quantum dot solar cells.

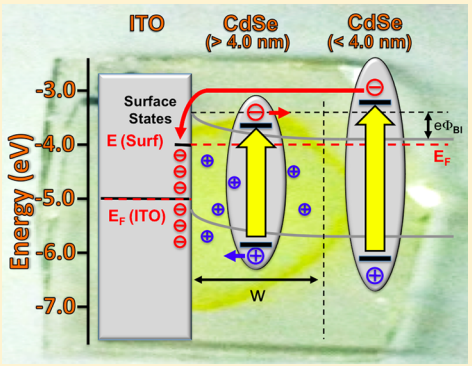

The quantum size effect is the basis for applications of CdSe quantum dots in third-generation solar cells,[1−6] photoelectrochemical cells,[7−10] photocatalysts,[11−15] and fluorescent labels. The size-dependent energetics of quantum dots control photochemical charge transfer,[16−25] photovoltage,[19,26−30] and hydrogen evolution.[31−34] Quantum dot solar cells employ nanocrystals as films sandwiched between electron- or hole-selective materials.[4,35] In hybrid solar cells,[3,36] the dots are mixed with organic polymers to aid light absorption and charge separation. Photochemical charge separation, transport, and recombination are key to the performance of these devices, but the details of these processes are often not fully understood.[6,35−37] Also, usually fully assembled devices are required for a characterization of these processes.[38]

Here we employ surface photovoltage spectroscopy (SPS) to observe the intrinsic photochemistry of CdSe nanocrystals in easy to fabricate drop-cast films in the absence of an external bias or added redox reagents. SPS is a contactless technique that probes contact potential difference changes (ΔCPD) in semiconductors, molecular light absorbers,[39,40] and nanocrystals[40−42] upon excitation with light (Figure 1).[43,44] The sensitivity of SPS is much higher than that of photoelectrochemistry,[45] thus allowing the detection of majority carrier type,[46] mid-gap states,[47,48] defects,[49] and electrochemical reactions at interfaces.[50] Measurements are typically performed in vacuum on sample films deposited onto metallic

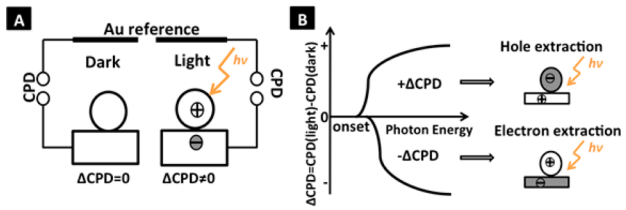

Figure 1. (A) Schematic configuration used for SPS measurement and (B) example spectra for electron and hole injection into the FTO substrate.

or semiconducting substrates. Earlier SPS studies on CdSe nanocrystal films by Hodes et al. observed photovoltage influenced by the size of the dots,[29] their chemical history, and the ambient environment.[28] Photochemical charge separation in such films was attributed to "slanted bands" across the nanocrystal films, in analogy to the space charge layer in solid semiconductors. Differences in hole and electron diffusion rates were attributed to trap sites on the surface of the dots. This diffusive transport was described as a special case of a Dember effect.[51] Our measurements show that photovoltages in CdSe quantum dot (QD) films on indium tin oxide (ITO)

Received: July 17, 2016
Accepted: August 9, 2016

DOI: 10.1021/acs.jpclett.6b01569
J. Phys. Chem. Lett. 2016, 7, 3335−3340

are generated by two distinct mechanisms, either by photochemical electron injection from the QDs into the ITO substrate or by polarization of QD-based polaron pairs by an electrical field at the CdSe−ITO interface. Both processes are controlled by the built-in voltage at the CdSe−ITO interface, degree of quantum confinement in the dots, and thickness of the films.

The interfacial electric field extends 150 nm into the QD film and causes a 0.3 eV potential barrier that repels electrons from the interface, based on SPS data on films with variable thickness. This explains why the effects of this space charge layer are most strongly felt in thin films and in films of the large dots. All of these effects can be understood on the basis of the thermodynamics of the ITO−CdSe QE system. Overall, this work sheds new light onto the factors that control photochemical charge transport and separation in CdSe QD films. These findings are relevant to the understanding of nanocrystal photoelectrochemical cells and third-generation photovoltaic devices.

2-mercaptoethanol-ligated CdSe quantum dots in the 2.0−4.2 nm size range were prepared by coprecipitation of cadmium perchlorate and sodium hydrogen selenide in water, according to the protocol by Weller and co-workers,[52] followed by size-selective precipitation with 2-propanol as the nonsolvent (Figure S1). UV−vis spectra of the CdSe QD fractions in water (Figure 2A) show a systematic variation of absorption edge. The sizes of the dots were obtained by estimation of the absorption edges using the approach by Weller and co-workers[53] and are listed in Table 1 together with other photophysical data. Films of the CdSe dots were then made by drop casting of the aqueous solution onto ITO-coated glass slides followed by drying in air. On the basis of profilometry data, the thickness of these films is 150 ± 20 nm. The absorption edge for each of the films is observed at 40−60 nm lower wavelength, compared to the solution. Similar red shifts have been observed by others and are generally attributed to a combination of optical scattering effects and dipolar coupling between the QDs in the films.[54−57] As will be shown below, SPS can be helpful in determining the effective band gap of such films.

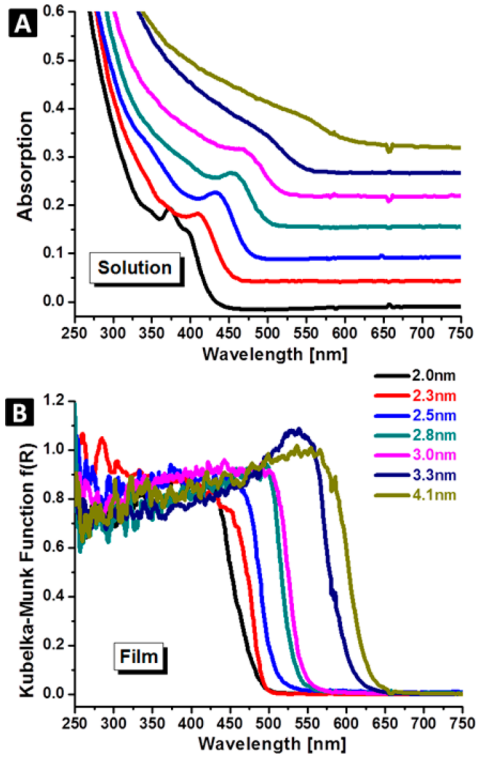

Figure 2. (A) Absorption spectra of CdSe QDs dispersions in water and (B) diffuse reflectance spectra of CdSe QDs films. QD diameters obtained by the Weller approach are shown in the legend[53] and in Table 1 together with other photophysical data.

Figure 3 shows surface photovoltage and diffuse reflectance ultraviolet−visible (UV−vis) spectra for a film made of 2.3 nm quantum dots. A negative photovoltage develops above 2.6 eV and reaches a maximum of −0.58 V at 3.6 eV. The onset at 0.2 eV *above* the optical absorption edge suggests the photovoltage is associated with the generation of free charge carriers in the CdSe dots. The negative sign of the voltage suggests the photoelectrons inject from the QD film into the ITO substrate, as seen previously for other nanocrystalline metal oxides.[46,50,58] The time constant for this process can be estimated with the transient photovoltage signal in the inset of Figure 3A. Under 3.75 eV illumination (0.1 mW cm^{-2}), 63.2% of the photovoltage maximum is reached after 8.1 s. A second type of behavior is observed for QDs with diameters above 4.0 nm (Figure 3B and Figure S2). Here the photovoltage is positive and small (+125 mV for the 4.2 nm and +80 mV for the 4.09 nm dots) and occurs approximately 0.2 eV *below* the optical band gap. The inversion of the voltage sign suggests that a different charge separation mechanism is operational in films of the larger dots. To rationalize these findings we employ the model in Figure 4. The diagram shows the band edges for two representative quantum dots sizes on a ITO support. Illumination generates electron hole pairs in the dots, of which the electrons can inject into the ITO support only if their electrochemical potential is sufficient to overcome the built-in potential barrier φ_{bi} at the interface. This applies to the <4.0 nm QDs, whose conduction band edge is elevated because of the quantum confinement effect.[34]

The electrostatic barrier results from the electric double layer that forms at the CdSe−ITO interface as a result of electron transfer from CdSe to ITO. The theoretical potential drop (the built-in potential) is given by the difference of Fermi levels of both phases, according to eq 1.

$$e\varphi_{bi} = E_F(\mathrm{CdSe}) - E_F(\mathrm{ITO}) \quad (1)$$

Photoelectrons created in the larger, less quantum-confined dots cannot overcome the potential barrier. In these dots the charge carriers form *polaron pairs* that are polarized under the influence of the space charge layer (small arrows in Figure 4). This process is analogous to films of organic semiconductors, which produce localized polaron pairs under sub-band gap excitation.[47,48,59] This model is supported by thickness-dependent SPS data for CdSe dots of intermediate size and 2.3 eV band gap (Figure 5). These films produce a photovoltage signal that depends strongly on the film thickness. Thin films (70 nm) yield a positive photovoltage, while thick films (700 nm) give a negative photovoltage signal under band gap excitation. A photovoltage sign inversion from negative to positive is observed for a film of intermediate thickness (150 nm). According to the model in Figure 4, the initial negative voltage is from free electron injection under 2.3 to 3.1 eV excitation, followed by repulsion of electrons under excitation at >3.2 eV. The repulsion is due to the increase of the depletion layer during the initial excitation period. On the basis of the

DOI: 10.1021/acs.jpclett.6b01569
J. Phys. Chem. Lett. 2016, 7, 3335−3340

Table 1. Summary of Optical and Photovoltage Data

diameter (nm)	2	2.3	2.4	2.5	2.8	3.2	3.3	4.1	4.2	bulk
E_G (Solution) (eV)	2.91	2.75	2.7	2.59	2.49	2.29	2.28	2.05	2.03	1.74
E_G (Film) (eV)	2.46	2.47	2.47	2.32	2.26	2.08	1.96	1.92	1.97	1.61
photo-onset (eV)	2.75	2.63	2.5	2.47	2.39	2.26	2.27	1.87	1.93	1.75
ΔCPD_{max} (V)	−0.4	−0.58	−0.75	−0.22	−0.34	−0.125	−0.25	0.08	0.125	0.0 ± 0.02
E_F (CdSe) (V) vs NHE[a]	−1.36	−1.3	−1.26	−1.21	−1.13	–	–	−0.75	−0.72	−0.51
E_F (CdSe) − E_F (ITO)	−1.76	−1.7	−1.66	−1.61	−1.53	–	–	−1.15	−1.12	−0.91

[a]From Zhao et al.[34]

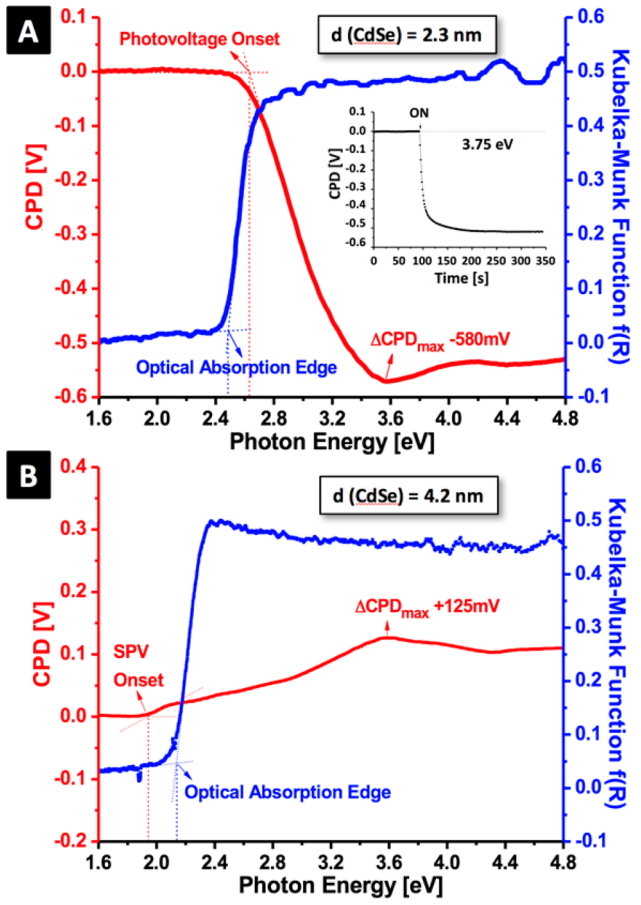

Figure 3. Surface photovoltage and optical absorption spectra of (A) 2.3 nm and (B) 4.2 nm QDs. Inset: transient photovoltage signal under 3.75 eV illumination of a 150 nm thick film of 2.3 nm dots.

photovoltage inversion in Figure 5, the depletion layer width, w, is estimated to be between 70 and 150 nm. This is larger than what has been postulated for a CdSe QD−Au junction (7.8 nm)[46] but similar to what has been measured for ITO/CdSe−P3HT contacts (30−40 nm).[60]

Because the maximum positive photovoltage for the 70 nm CdSe QD film in Figure 5 is caused by electrostatic repulsion, its numerical value can be used to estimate the built-in potential of the ITO−CdSe configuration $\Delta CPD = \varphi_{Bi} = +0.45$ V. The true value of φ_{Bi} may be higher because the electrostatic potential decays exponentially with distance from the interface. For an ideal Schottky junction, $e\varphi_{Bi}$ is given by eq 1. Using E_F(ITO) = +0.40 V vs NHE,[46] and E_F(CdSe) values from photoelectrochemistry measurements,[34] one calculates $e\varphi_{Bi}$ = +1.76 eV for dots with E_G = 2.9 eV and E_F = −1.36 V (vs NHE),[34] and $e\varphi_{Bi}$ = +1.15 eV for dots with E_G = 2.05 eV and E_F = −0.75 V (vs NHE).[34] These values are 0.7−1.3 eV higher

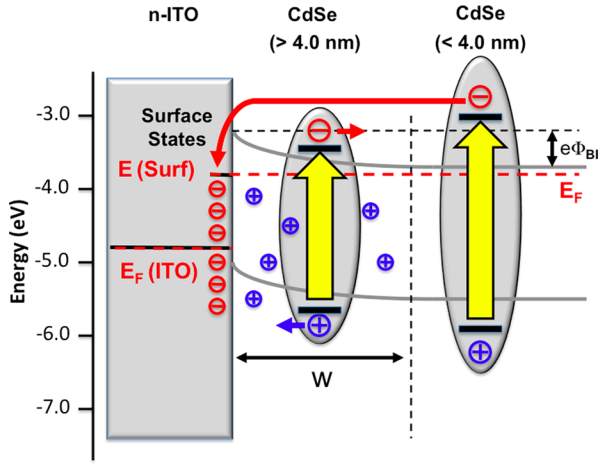

Figure 4. Schematic energy levels and electrostatic potential at the ITO−CdSe interface. The band bending $e\Phi_{Bi}$ in the space charge layer is due to the electrochemical equilibrium between ITO surface states E_F(surface) and E_F(CdSe). The value for φ_{bi} may also be further modified by dipoles at the ITO−CdSe interface, caused for example by ligand absorption.[61]

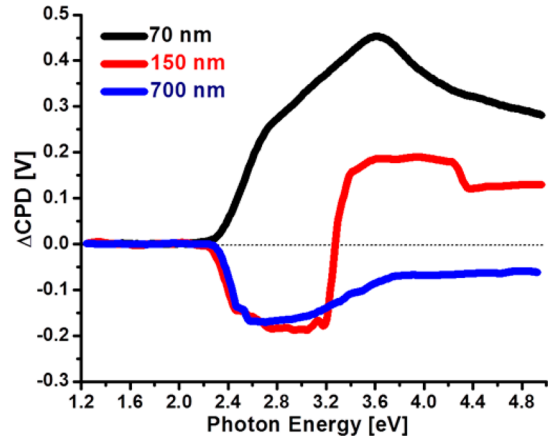

Figure 5. Surface photovoltage spectra for CdSe QDs films (band gap 2.3 eV) with variable thickness (70−700 nm).

than the experimental value of +0.45 eV. This observation agrees with other CdS systems reported in the literature. For example, low $e\varphi_{Bi}$ values have been observed for junctions between CdSe and Au (+0.27 eV)[62] and for ITO/SnO_2 and CdS/CdTe junctions (+1.1 and +0.95 eV, respectively).[63] These discrepancies are likely due to Fermi pinning caused by chemical reactions at the QD−ITO interface, which modify the workfunction of ITO and CdSe.[64] In the present case such states could result from the reaction of In^{3+} or Sn^{4+} ions at the ITO surface with Se^{2-} ions from the quantum dots.

DOI: 10.1021/acs.jpclett.6b01569
J. Phys. Chem. Lett. 2016, 7, 3335−3340

Next we turn our attention to the dependence of the absolute values of the photovoltage maxima on the size of the dots and their optical band gaps. As can be seen in Figure 6, there is a

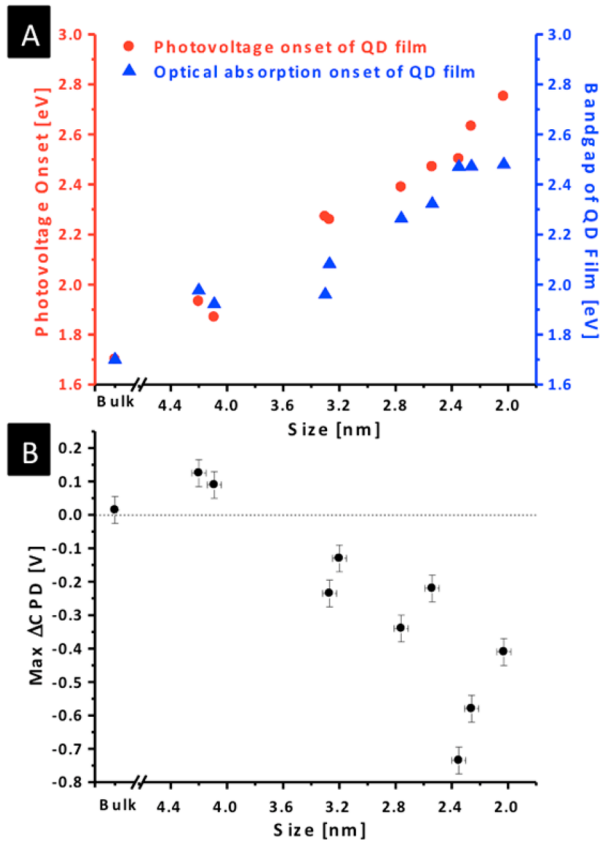

Figure 6. (A) Plot of surface photovoltage onset energy (eV) and film band gap versus nanoparticle diameter. (B) Maximum photovoltage versus QD band gap. Deviations of individual data from the trend are due to variations in film thickness (150 ± 20 nm).

monotonic increase of the maximum photovoltage voltage with decreasing size of the quantum dots. This trend is further analyzed in Figure 7 as a function of the QD band gaps and the QD quasi Fermi energies.

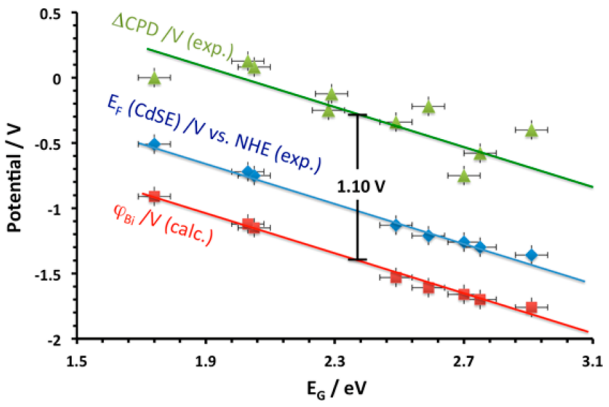

Figure 7. Relationship between QD band gap (in solution), experimental photovoltage maxima, quasi Fermi energies from photoelectrochemical onset potentials,[34] and built-in potential (from eq 1 with E_F(ITO) = +0.40 V vs NHE). Values are given in Table 1.

The experimental photovoltages show an approximately linear increase with the QD band gaps. This dependence is expected from thermodynamics: As the band gap expands, the conduction band edge and the Fermi levels of the dots (second line graph)[34] become more reducing, which increases the built-in potential (third line graph) of the ITO−CdSe configuration. As can be seen in Figure 7, the experimental photovoltage values for the measured QD films are on average 1.1 V less negative than the theoretical values for $e\varphi_{Bi}$, based on an ideal Schottky junction. This agrees well with the 0.7−1.3 V shortfall as discussed above and further confirms the presence of ITO−CdSe interfacial states (Fermi level pinning) approximately 1.1 eV above the ITO Fermi level (Figure 4).

Lastly, we discuss the correlation between the photovoltage onset energy and the optical band gap in the QD films. According to the data in Figure 6A and Table 1, films made of the large dots (>4.0 nm) show a photovoltage onset that is *smaller* than the optical band gaps of both the film and the solution. For these films, the photovoltage signal is due to the polarization of localized polaron pairs. The low photo-onset can be explained by assuming that some of these polaron pairs reside in subgap trap states that are likely present on the surface of the quantum dots.[65] Based on the photovoltage spectra, these states are 0.10−0.18 eV below the QD band gap. In contrast, films made of the small dots (<4.0 nm) have a photovoltage onset energy *above* the optical band gaps for the films and *below* the optical band gap for the dissolved dots. Because the photovoltage signal is due to the movement of free carriers, the photo-onset energy can be taken as the *effective band gap*, E_{Eff}, of the film. The reduction of E_{Eff} by 0.01−0.20 eV with regard to the optical band gap of the *free* dots can be attributed to dipolar coupling interactions between adjacent dots and the associated change in dielectric constant in the films.[54−57] Thus, the SPS data allows a differentiation between dielectric effects on the optical band gap of the QDs films and the effect of subgap trap states.

On the basis of SPS, the CdSe quantum dots form a Schottky junction with ITO. A photovoltage can result from majority carrier injection into the ITO substrate and/or from polarization of electron−hole pairs by the electric field in the space charge layer. The relatively low built-in potential of 0.45 V is attributed to the formation of In−Se interfacial states 1.1 V negative of the ITO conduction band (Fermi level pinning). Thickness-dependent SPS estimates the space charge layer width between 70 and 150 nm. The effective band gap of the QD films is observed between the optical band gaps of the dispersed dots and that of the films. The difference is due to dipolar coupling between QDs in the films. Additionally, subgap states are detected in the SPV onsets for the large dots (>4.0 nm). These states are 0.10−0.18 eV below the optical band gap of the dispersed dots and might arise from covalent interactions between the QDs or between the QDs and the ligands. The ability of SPS to observe effective band gaps, subband gap states, space charge layer width, and built-in potentials is thought to be useful for the development of quantum dot photovoltaic devices.

EXPERIMENTAL SECTION

Synthesis. Mercaptoethanol-ligated CdSe quantum dots in the 2.0−5.0 nm size range were synthesized using the protocol reported by Rogach et al.[52] Size-selective precipitation with isopropanol was performed to obtain nanocrystals with different sizes as described before.[34] QDs were dispersed in

DOI: 10.1021/acs.jpclett.6b01569
J. Phys. Chem. Lett. 2016, 7, 3335−3340

water for UV−vis measurements in solution. The size of the QDs was determined from their optical band gap using a relation given by Schooss et al.[53] CdSe films for SPS measurements were prepared by dropcasting 1.0 mg/mL aqueous solution of CdSe nanocrystals on tin-doped indium oxide substrates, followed by air-drying overnight in the dark. Unless stated otherwise, the thickness of CdSe films was kept consistent (150 ± 20 nm) among various sizes of dots, as characterized by a Dektak surface profilometer.

UV−vis spectroscopy was performed on film samples prepared by dropcoating onto a glass slide covered with Teflon tape. The absorption spectra of the solutions and the diffuse reflectance spectra of the film were collected using an Ocean Optics DH2000 deuterium and halogen light source and HR2000 CG UV-vis-NIR spectrometer. Surface photovoltage spectroscopy was performed under vacuum ($<3 \times 10^{-4}$ mbar) using a home-built vacuum chamber and a commercial, semitransparent Kelvin probe (Delta PHI Besocke) at 1 mm sample−probe distance. Samples were illuminated from the top through a quartz window using monochromatic light scanned from 1000 to 250 nm with a peak width of 30 nm produced by a Cornerstone 130 monochromator powered by a 175W Xe arc lamp. The light intensity at the sample was 0.1−0.5 mW cm^{-2}. The spectra acquisition time is 625 s, well above the time constant of the experiment (8.1 s, based on the evolution of the largest photovoltage signal in the inset of Figure 3A).

■ ASSOCIATED CONTENT

Supporting Information

The Supporting Information is available free of charge on the ACS Publications website at DOI: 10.1021/acs.jpclett.6b01569.

Photos of CdSe QD samples of various sizes and representative SPV spectra (PDF)

■ AUTHOR INFORMATION

Corresponding Author

*Fax: 530 752 8995. Tel: 540 754 6242. E-mail: fosterloh@ucdavis.edu.

Notes

The authors declare no competing financial interest.

■ ACKNOWLEDGMENTS

This material is based upon work supported by the U.S. Department of Energy, Office of Science, Office of Basic Energy Sciences under Award Number DE-SC-0001234 and Research Corporation for Science Advancement (Scialog award). We thank Adam Moulé for access to the profilometer.

■ REFERENCES

(1) Huynh, W. U.; Dittmer, J. J.; Alivisatos, A. P. Hybrid nanorod-polymer solar cells. *Science* **2002**, *295* (5564), 2425−2427.

(2) Hodes, G.; Howell, I. D. J.; Peter, L. M.; Nanocrystalline Photoelectrochemical. Cells - A New Concept In Photovoltaic Cells. *J. Electrochem. Soc.* **1992**, *139* (11), 3136−3140.

(3) Huynh, W. U.; Peng, X. G.; Alivisatos, A. P. CdSe nanocrystal rods/poly(3-hexylthiophene) composite photovoltaic devices. *Adv. Mater.* **1999**, *11* (11), 923.

(4) Gur, I.; Fromer, N. A.; Geier, M. L.; Alivisatos, A. P. Air-stable all-inorganic nanocrystal solar cells processed from solution. *Science* **2005**, *310* (5747), 462−465.

(5) Leschkies, K. S.; Divakar, R.; Basu, J.; Enache-Pommer, E.; Boercker, J. E.; Carter, C. B.; Kortshagen, U. R.; Norris, D. J.; Aydil, E. S. Photosensitization of ZnO nanowires with CdSe quantum dots for photovoltaic devices. *Nano Lett.* **2007**, *7* (6), 1793−1798.

(6) Greaney, M. J.; Couderc, E.; Zhao, J.; Nail, B. A.; Mecklenburg, M.; Thornbury, W.; Osterloh, F. E.; Bradforth, S. E.; Brutchey, R. L. Controlling the Trap State Landscape of Colloidal CdSe Nanocrystals with Cadmium Halide Ligands. *Chem. Mater.* **2015**, *27* (3), 744−756.

(7) Wang, G. M.; Yang, X. Y.; Qian, F.; Zhang, J. Z.; Li, Y. Double-Sided CdS and CdSe Quantum Dot Co-Sensitized ZnO Nanowire Arrays for Photoelectrochemical Hydrogen Generation. *Nano Lett.* **2010**, *10* (3), 1088−1092.

(8) Frese, K. W. Electrochemical studies of photocorrosion of n-CdSe. *J. Electrochem. Soc.* **1983**, *130* (1), 28−33.

(9) Harris, D.; Winnick, J.; Kohl, P. A. Cation Effect on the CdSe-Liquid Junction. *J. Electrochem. Soc.* **1993**, *140* (9), 2581−2588.

(10) Webber, D. H.; Brutchey, R. L. Ligand Exchange on Colloidal CdSe Nanocrystals Using Thermally Labile tert-Butylthiol for Improved Photocurrent in Nanocrystal Films. *J. Am. Chem. Soc.* **2012**, *134* (2), 1085−1092.

(11) Maruska, H. P.; Ghosh, A. K. Photocatalytic Decomposition of Water at Semiconductor Electrodes. *Sol. Energy* **1978**, *20* (6), 443−458.

(12) Kambe, S.; Fujii, M.; Kawai, T.; Kawai, S.; Nakahara, F. Photocatalytic Hydrogen-Production with Cd(S, Se) Solid-Solution Particles - Determining Factors for the Highly Efficient Photocatalyst. *Chem. Phys. Lett.* **1984**, *109* (1), 105−109.

(13) Jing, D. W.; Guo, L. J. A novel method for the preparation of a highly stable and active CdS photocatalyst with a special surface nanostructure. *J. Phys. Chem. B* **2006**, *110* (23), 11139−11145.

(14) Amirav, L.; Alivisatos, A. P. Photocatalytic Hydrogen Production with Tunable Nanorod Heterostructures. *J. Phys. Chem. Lett.* **2010**, *1* (7), 1051−1054.

(15) Yang, S. Y.; Prendergast, D.; Neaton, J. B. Tuning Semiconductor Band Edge Energies for Solar Photocatalysis via Surface Ligand Passivation. *Nano Lett.* **2012**, *12* (1), 383−388.

(16) Burda, C.; El-Sayed, M. A. High-density femtosecond transient absorption spectroscopy of semiconductor nanoparticles. A tool to investigate surface quality. *Pure Appl. Chem.* **2000**, *72* (1−2), 165−177.

(17) Robel, I.; Subramanian, V.; Kuno, M.; Kamat, P. V. Quantum dot solar cells. Harvesting light energy with CdSe nanocrystals molecularly linked to mesoscopic TiO2 films. *J. Am. Chem. Soc.* **2006**, *128* (7), 2385−2393.

(18) Robel, I.; Kuno, M.; Kamat, P. V. Size-dependent electron injection from excited CdSe quantum dots into TiO2 nanoparticles. *J. Am. Chem. Soc.* **2007**, *129* (14), 4136−4137.

(19) Gross, D.; Mora-Sero, I.; Dittrich, T.; Belaidi, A.; Mauser, C.; Houtepen, A. J.; Da Como, E.; Rogach, A. L.; Feldmann, J. Charge Separation in Type II Tunneling Multi layered Structures of CdTe and CdSe Nanocrystals Directly Proven by Surface Photovoltage Spectroscopy. *J. Am. Chem. Soc.* **2010**, *132* (17), 5981−5983.

(20) Bang, J. H.; Kamat, P. V. CdSe Quantum Dot-Fullerene Hybrid Nanocomposite for Solar Energy Conversion: Electron Transfer and Photoelectrochemistry. *ACS Nano* **2011**, *5* (12), 9421−9427.

(21) Chuang, C. H.; Doane, T. L.; Lo, S. S.; Scholes, G. D.; Burda, C. Measuring Electron and Hole Transfer in Core/Shell Nanoheterostructures. *ACS Nano* **2011**, *5* (7), 6016−6024.

(22) Tvrdy, K.; Frantsuzov, P. A.; Kamat, P. V. Photoinduced electron transfer from semiconductor quantum dots to metal oxide nanoparticles. *Proc. Natl. Acad. Sci. U. S. A.* **2011**, *108* (1), 29−34.

(23) Jones, M.; Lo, S. S.; Scholes, G. D. Quantitative modeling of the role of surface traps in CdSe/CdS/ZnS nanocrystal photoluminescence decay dynamics. *Proc. Natl. Acad. Sci. U. S. A.* **2009**, *106* (9), 3011−3016.

(24) Wilker, M. B.; Schnitzenbaumer, K. J.; Dukovic, G. Recent Progress in Photocatalysis Mediated by Colloidal II-VI Nanocrystals. *Isr. J. Chem.* **2012**, *52* (11−12), 1002−1015.

(25) Brus, L. E. AA Simple-Model for the Ionization-Potential, Electron-Affinity, and Aqueous Redox Potentials of Small Semiconductor Crystallites. *J. Chem. Phys.* **1983**, *79* (11), 5566−5571.

DOI: 10.1021/acs.jpclett.6b01569
J. Phys. Chem. Lett. 2016, 7, 3335−3340

(26) Brillson, L. J. Surface Photovoltage and Electron Energy-Loss Spectroscopy of Oxygen Adsorbed on (1120) CdSe. *J. Vac. Sci. Technol.* **1976**, *13* (1), 325−328.
(27) Hodes, G. Size-Quantized Nanocrystalline Semiconductor-Films. *Isr. J. Chem.* **1993**, *33* (1), 95−106.
(28) Kronik, L.; Ashkenasy, N.; Leibovitch, M.; Fefer, E.; Yoram, S.; Gorer, S.; Hodes, G. Surface States and Photovoltaic Effects in CdSe Quantum Dot Films. *J. Electrochem. Soc.* **1998**, *145* (5), 1748−1755.
(29) Gal, D.; Mastai, Y.; Hodes, G.; Kronik, L. Band gap determination of semiconductor powders via surface photovoltage spectroscopy. *J. Appl. Phys.* **1999**, *86* (10), 5573−5577.
(30) Zaniewski, A. M.; Loster, M.; Sadtler, B.; Alivisatos, A. P.; Zettl, A. Direct measurement of the built-in potential in a nanoscale heterostructure. *Phys. Rev. B: Condens. Matter Mater. Phys.* **2010**, *82* (15), 155311.
(31) Frame, F. A.; Carroll, E. C.; Larsen, D. S.; Sarahan, M. S.; Browning, N. D.; Osterloh, F. E. First demonstration of CdSe as a photocatalyst for hydrogen evolution from water under UV and visible light. *Chem. Commun.* **2008**, 2206−2208.
(32) Frame, F. A.; Osterloh, F. E. CdSe-MoS_2: A Quantum Size-Confined Photocatalyst for Hydrogen Evolution from Water under Visible Light. *J. Phys. Chem. C* **2010**, *114*, 10628−10633.
(33) Holmes, M. A.; Townsend, T. K.; Osterloh, F. E. Quantum confinement controlled photocatalytic water splitting by suspended CdSe nanocrystals. *Chem. Commun.* **2012**, *48* (3), 371−373.
(34) Zhao, J.; Holmes, M. A.; Osterloh, F. E. Quantum Confinement Controls Photocatalysis - A Free Energy Analysis for Photocatalytic Proton Reduction at CdSe Nanocrystals. *ACS Nano* **2013**, *7* (5), 4316−4325.
(35) Luther, J. M.; Law, M.; Beard, M. C.; Song, Q.; Reese, M. O.; Ellingson, R. J.; Nozik, A. J. Schottky Solar Cells Based on Colloidal Nanocrystal Films. *Nano Lett.* **2008**, *8* (10), 3488−3492.
(36) Greaney, M. J.; Brutchey, R. L. Ligand engineering in hybrid polymer:nanocrystal solar cells. *Mater. Today* **2015**, *18*, 31.
(37) Antunez, P. D.; Buckley, J. J.; Brutchey, R. L. Tin and germanium monochalcogenide IV-VI semiconductor nanocrystals for use in solar cells. *Nanoscale* **2011**, *3* (6), 2399−2411.
(38) Gao, J.; Zhang, J.; van de Lagemaat, J.; Johnson, J. C.; Beard, M. C. Charge Generation in PbS Quantum Dot Solar Cells Characterized by Temperature-Dependent Steady-State Photoluminescence. *ACS Nano* **2014**, *8* (12), 12814−12825.
(39) Fungo, F.; Milanesio, M. E.; Durantini, E. N.; Otero, L.; Dittrich, T. Optically induced switch of the surface work function in TiO2/porphyrin-C-60 dyad system. *J. Mater. Chem.* **2007**, *17* (20), 2107−2112.
(40) Mora-Sero, I.; Dittrich, T.; Susha, A. S.; Rogach, A. L.; Bisquert, J. Large improvement of electron extraction from CdSe quantum dots into a TiO2 thin layer by N3 dye coabsorption. *Thin Solid Films* **2008**, *516* (20), 6994−6998.
(41) Mora-Sero, I.; Bisquert, J.; Dittrich, T.; Belaidi, A.; Susha, A. S.; Rogach, A. L. Photosensitization of TiO2 layers with CdSe quantum dots: Correlation between light absorption and photoinjection. *J. Phys. Chem. C* **2007**, *111* (40), 14889−14892.
(42) Zillner, E.; Dittrich, T. Surface photovoltage within a monolayer of CdSe quantum dots. *Phys. Status Solidi RRL* **2011**, *5* (7), 256−258.
(43) Kronik, L.; Shapira, Y. Surface Photovoltage Phenomena: Theory, Experiment, and Applications. *Surf. Sci. Rep.* **1999**, *37* (1−5), 1−206.
(44) Kronik, L.; Shapira, Y. Surface Photovoltage Spectroscopy of Semiconductor Structures: At the Crossroads of Physics, Chemistry and Electrical Engineering. *Surf. Interface Anal.* **2001**, *31* (10), 954−965.
(45) Lagowski, J. Semiconductor Surface Spectroscopies - The Early Years. *Surf. Sci.* **1994**, *299-300* (1−3), 92−101.
(46) Yang, Y.; Wang, J.; Zhao, J.; Nail, B. A.; Yuan, X.; Guo, Y.; Osterloh, F. E. Photochemical Charge Separation at Particle Interfaces: The n-BiVO4−p-Silicon System. *ACS Appl. Mater. Interfaces* **2015**, *7* (10), 5959−5964.
(47) Osterloh, F. E.; Holmes, M. A.; Zhao, J.; Chang, L.; Kawula, S.; Roehling, J. D.; Moulé, A. J. P3HT:PCBM Bulk-Heterojunctions: Observing Interfacial and Charge Transfer States with Surface Photovoltage Spectroscopy. *J. Phys. Chem. C* **2014**, *118* (27), 14723−14731.
(48) Osterloh, F. E.; Holmes, M. A.; Chang, L.; Moule, A. J.; Zhao, J. Photochemical Charge Separation in Poly(3-hexylthiophene) (P3HT) Films Observed with Surface Photovoltage Spectroscopy. *J. Phys. Chem. C* **2013**, *117* (51), 26905−26913.
(49) Wu, P.; Wang, J.; Zhao, J.; Guo, L.; Osterloh, F. E. Structure defects in g-C3N4 limit visible light driven hydrogen evolution and photovoltage. *J. Mater. Chem. A* **2014**, *2* (47), 20338−20344.
(50) Wang, J.; Zhao, J.; Osterloh, F. E. Photochemical charge transfer observed in nanoscale hydrogen evolving photocatalysts using surface photovoltage spectroscopy. *Energy Environ. Sci.* **2015**, *8*, 2970−2976.
(51) Dember, H. A photoelectrical-motor energy in copper-oxide crystals. *Phys. Z.* **1931**, *32*, 554−556.
(52) Rogach, A. L.; Kornowski, A.; Gao, M. Y.; Eychmuller, A.; Weller, H. Synthesis and characterization of a size series of extremely small thiol-stabilized CdSe nanocrystals. *J. Phys. Chem. B* **1999**, *103* (16), 3065−3069.
(53) Schooss, D.; Mews, A.; Eychmuller, A.; Weller, H. Quantum-Dot Quantum-Well CdS/HgS/CdS - Theory and Experiment. *Phys. Rev. B: Condens. Matter Mater. Phys.* **1994**, *49* (24), 17072−17078.
(54) Rabani, E.; Hetenyi, B.; Berne, B. J.; Brus, L. E. Electronic properties of CdSe nanocrystals in the absence and presence of a dielectric medium. *J. Chem. Phys.* **1999**, *110* (11), 5355−5369.
(55) Dollefeld, H.; Weller, H.; Eychmuller, A. Semiconductor nanocrystal assemblies: Experimental pitfalls and a simple model of particle-particle interaction. *J. Phys. Chem. B* **2002**, *106* (22), 5604−5608.
(56) Schedelbeck, G.; Wegscheider, W.; Bichler, M.; Abstreiter, G. Coupled quantum dots fabricated by cleaved edge overgrowth: From artificial atoms to molecules. *Science* **1997**, *278* (5344), 1792−1795.
(57) Yoffe, A. D. Semiconductor quantum dots and related systems: electronic, optical, luminescence and related properties of low dimensional systems. *Adv. Phys.* **2001**, *50* (1), 1−208.
(58) Zhao, J.; Osterloh, F. E. Photochemical Charge Separation in Nanocrystal Photocatalyst Films − Insights from Surface Photovoltage Spectroscopy. *J. Phys. Chem. Lett.* **2014**, *5*, 782−786.
(59) Chamousis, R. L.; Chang, L.; Watterson, W. J.; Montgomery, R. D.; Taylor, R. P.; Moule, A. J.; Shaheen, S. E.; Ilan, B.; van de Lagemaat, J.; Osterloh, F. E. Effect of Fractal Silver Electrodes on Charge Collection and Light Distribution in Semiconducting Organic Polymer Films. *J. Mater. Chem. A* **2014**, *2* (39), 16608−16616.
(60) Ramar, M.; Suman, C. K.; Manimozhi, R.; Ahamad, R.; Srivastava, R. Study of Schottky contact in binary and ternary hybrid CdSe quantum dot solar cells. *RSC Adv.* **2014**, *4* (62), 32651−32657.
(61) Bruening, M.; Moons, E.; Yaronmarcovich, D.; Cahen, D.; Libman, J.; Shanzer, A. Polar Ligand Adsorption Controls Semiconductor Surface-Potentials. *J. Am. Chem. Soc.* **1994**, *116* (7), 2972−2977.
(62) Sarangi, S. N.; Adhikari, P. K.; Pandey, D.; Sahu, S. N. Current-voltage and capacitance-voltage studies of nanocrystalline CdSe/Au Schottky junction interface. *J. Nanopart. Res.* **2010**, *12* (6), 2277−2286.
(63) Das, S. K.; Morris, G. C. Preparation and Properties of Electrodeposited Indium Tin Oxide/Sno2/Cdte and Indium Tin Oxide/SnO2/CdS/CdTe Solar-Cells. *J. Appl. Phys.* **1993**, *73* (2), 782−786.
(64) Boettcher, S. W.; Strandwitz, N. C.; Schierhorn, M.; Lock, N.; Lonergan, M. C.; Stucky, G. D. Tunable electronic interfaces between bulk semiconductors and ligand-stabilized nanoparticle assemblies. *Nat. Mater.* **2007**, *6* (8), 592−596.
(65) Law, M.; Luther, J. M.; Song, O.; Hughes, B. K.; Perkins, C. L.; Nozik, A. J. Structural, optical, and electrical properties of PbSe nanocrystal solids treated thermally or with simple amines. *J. Am. Chem. Soc.* **2008**, *130* (18), 5974−5985.

DOI: 10.1021/acs.jpclett.6b01569
J. Phys. Chem. Lett. 2016, 7, 3335−3340